The 10th JFPS International Symposium on Fluid Power FUKUOKA 2017 Oct. 24-27, 2017 The Japan Fluid Power System Society

Structure Design of a New Intelligent Pipeline Plugging Device

Wu Tingting*, Zhao Hong**

* College of Mechanical and Transportation Engineering, China University of Petroleum (Beijing), 102249, Beijing, China
18 Fuxue Road, Changping, Beijing, 102249 China
(E-mail: ttabbmmjj@163.com)
** College of Mechanical and Transportation Engineering, China University of Petroleum (Beijing), 102249, Beijing, China
18 Fuxue Road, Changping, Beijing, 102249 China

Abstract. The high pressure and intelligent plugging in the tube is an emerging pipeline maintenance and repair technology. It has the advantages of simple process, short working time, high plugging pressure, safe, reliable, etc. Based on the plugging requirement of oil and gas pipelines with small aperture, a kind of isolation plugging tool (IPT) mechanism of pneumatic tendon has designed. The mechanical characteristics of the IPT have been optimized by analyzing the dynamic characteristic curve and stress characteristic of the locking process.
Keywords: Intelligent Pipeline Plugging; Plugging Process; Pneumatic Tendon; Dynamic Analysis; Durability Analysis

1 INTRODUCTION

The oil and gas pipelines are rapidly developed by means of safety, reliability, continuous smoothness, large quantity of transportation and automatic control. However, oil and gas pipelines are susceptible to factors such as load mutation, environmental corrosion and man-made damage, leading to the leakage of oil and natural gas, which is resulting in a huge environmental damage and economic losses. With the extension of the pipeline service life, especially into the 1990s, pipeline damage incidents have increased year by year. At the same time, due to pipeline transformation, man-made damage, natural disasters and other reasons, the pipeline often needs to be repaired, such as: valve replacement, increase slip, pipeline modification and pipe replacement, etc. Therefore, the safety and effectiveness of the maintenance and repair of pipelines have seriously affected the production and transportation safety of oil and gas [1].
The existing plugging technologies include: frozen plugging technology, non-stop with pressure hole plugging technology, the pipeline intelligent plugging technology [2-5]. Among them, the frozen plugging technology construction process is simple, safe and reliable, low cost, but the plugging pressure is low, poor adaptability to the external environment and brings construction risks. Non-stop with pressure hole plugging technology is active, more mature pipe blocking technology. The technology is mature, the construction of safe and reliable, to avoid economic losses due to stop the transmission of media or reduce the pressure. But its construction process is complex, blocking the cycle is long, and the need for holes in the pipeline for the subsequent operation of the pipeline to bring security risks, but also to the pipeline maintenance operations inconvenience. Intelligent plugging in the pipeline is a new pipeline repair and maintenance technology. The technology construction process with high plugging pressure and short operating time is simple, safe and reliable. So it belongs to the pipeline maintenance and repair operations which plays an increasingly important role.
Based on the high pressure and small diameter of the oil and gas pipelines, this paper designs a kind of intelligent pipeline plugging device with pneumatic tendon, and carries on the dynamic simulation and the durability analysis to optimize the plugging structure.

2 WORKING PRINCIPLE OF INTELLIGENT PIPELINE PLUGGING

The structure of the active IPT is shown in Figure 2.1 (a). It is mainly composed of mechanical locking mechanism, emergency treatment system, communication and control system and micro hydraulic system [6]. The working principle is shown in Figure 2.1 (b). When the plugging operation is performed, the IPT is put into the pipe from the serving end and moved along the pipeline as the pressure of the pipe conveying medium. The micro hydraulic system is triggered when the IPT reaches the point where it needs to be plugged and pushing the locking sliders to slide along the dovetail groove on the cone. The IPT brakes and plugs by friction between the locking sliders and inner wall of pipeline. The locking sliders squeeze the rubber sealing ring, make it contact with the inner wall of the pipeline achieve to realize sealing.
After the pipeline repair operation is completed, the unlocking device of the IPT is triggered. The friction force between the locking sliders and inner wall of pipeline disappears. The IPT continues to walk downstream, which is driven by the medium pressure in the pipeline, until it is removed from the receiving end. The friction

between the locking slider and the inner wall of the pipe is the only balance force to balance the delivery pressure in the tube. Therefore, the dynamic performance of the locking mechanism plays a decisive role in the blocking effect.

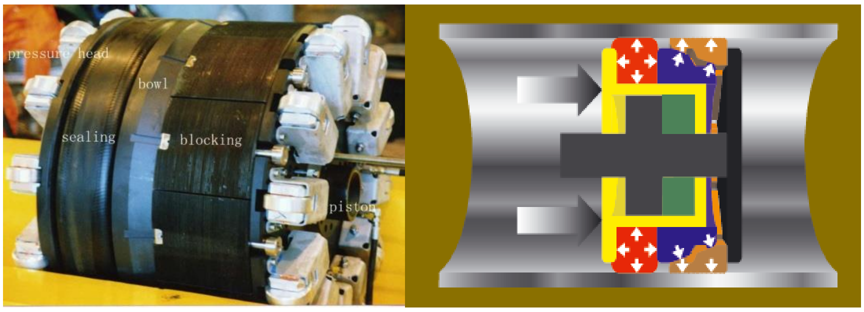

FIGURE 2.1 Intelligent High - Pressure Pipe Plugging and Working Principle
(a) Structure diagram (b) Schematic diagram

3 STRUCTURE DESIGN OF INTELLIGENT PIPELINE PLUGGING DEVICE BASED ON PNEUMATIC TENDON

3.1 Structural Design

As the hydraulic system design and working process is complex, they are prone to cause oil spills and environment pollution and other problems. This paper designs a kind of pipeline plugging device structure based on pneumatic tendon. The structure of the pipeline plugging device is shown in Fig. 3.1, mainly composed of left bearing block, cone, locking slider, push cylinder, right bearing block and pneumatic tendon. The plugging mechanism selected MXAM-20-AA type pneumatic tendon, the pneumatic control system to drive cone and pressure block movement. The braking and plugging action is achieved by the friction between the locking sliders and the inner wall of pipeline. The pneumatic system with micro-gas compressor provides air supply which largely simplifies the structure of the IPT.

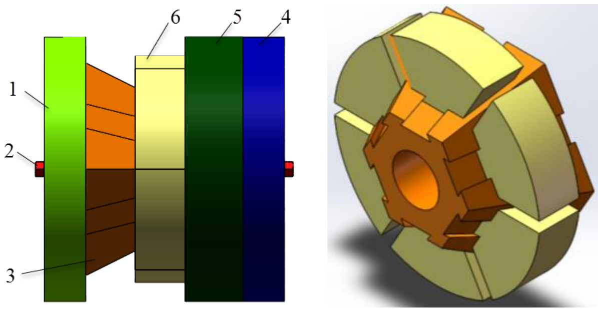

FIGURE 3.1 Intelligent Pipeline Plugging Structure
1-Left Bearing Block; 2-Pneumatic Tendon; 3-Cone; 4-Right Bearing Block; 5-Push Cylinder; 6-Locking Slider

During the plugging process, the isolation plugging tool and the fluid in the pipeline produce a mutual feedback effect. The dynamic analysis of the PIG model under different conditions shows that the mechanical parameters of the isolation tool have a great influence on the mutual feedback effect [8-13]. Minami and Shoham (1995) developed a dynamic model considering the length of the pig [14]. As shown in Figure 3.2, where d_1 has the greatest effect on the upstream and downstream differential pressure Δp, followed by d, L has the least effect [15]. Therefore, the parameters of the intelligent pipeline plugging structure are designed based on the Eq. (1), the optimization of genetic algorithm are utilized to obtain the size of d, d_1, and L.

$$\begin{aligned}\Delta p = {} & b_0 + b_1 L + b_2 d_1 + b_3 d + b_4 L^2 + b_5 d_1^2 + b_6 d^2 + b_7 \left(Ld\right) \\ & + b_8 \left(Ld_1\right) + b_9 \left(dd_1\right) + b_{10} \left(L^2 d_1\right) + b_{11} \left(d_1^2 d\right)\end{aligned} \tag{1}$$

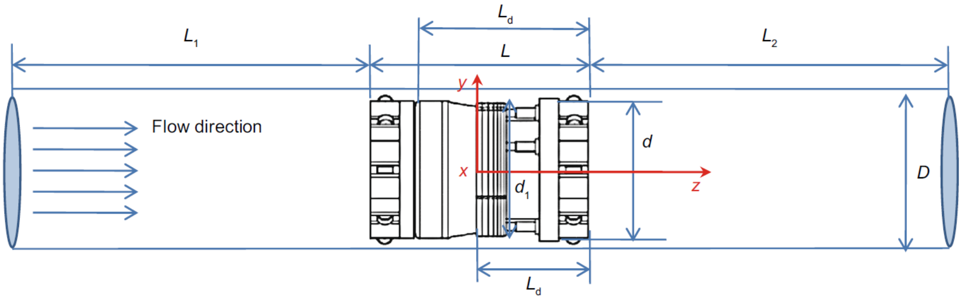

FIGURE 3.2 Intelligent Pipeline Plugging Structure in a Pipe

3.2 Principle of Operation

The pneumatic tendon is connected to the left bearing block and the right bearing block by its bolts at both ends, as shown in Figure 3.3 (a). At the beginning of the plugging operation, the compressor is working and the pneumatic tendon is contracted due to inflation. The left and right bearing blocks move in the direction of the pneumatic tendon force F, which are causing the push cylinder to push the locking slider to move along the dovetail groove along the cone. When the friction of the locking slider and the pipeline inner wall and pressure within the pipeline balance, the plug operation is completed, as shown in Figure 3.3 (b). After the plug operation is completed, the compressor pressure relief, pneumatic tendon to restore the original state and unlock complied.

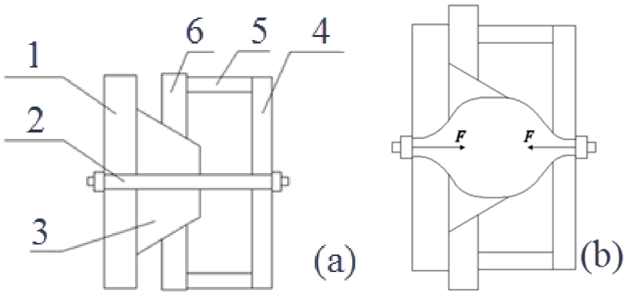

FIGURE 3.3 A Description of the IPT Mechanism
(a) Before plugging (b)After plugging
1-Left BearingBlock;2-Pneumatic Tendon;3-Cone; 4-Right Bearing Block;5-Push Cylinder;6-Locking Slider

3.3 Analysis of static characteristics of pneumatic tendon

In practice, the non-linear changes in pneumatic tendon are caused by the elasticity of the rubber tube and the internal friction of the pneumatic tendon. The more complete elastic mathematical model of the pneumatic tendon can be obtained by adding the rubber tube elastic force and the friction between the pneumatic tendon braid and the rubber tube.

$$F = PA - F_s \pm F_r \tag{2}$$

$$F_r = \mu N_f \tag{3}$$

$$F_s = Et_k D_0 [\frac{(1-\varepsilon)^2}{\tan^2\theta_0}(1-\frac{\sin\theta_0}{\sin\theta}) + \varepsilon\frac{\sin\theta}{\sin\theta_0}] \tag{4}$$

Among: E − Elastic Modulus of Pneumatic Tendon Rubber, Pa;

t_k − The thickness of the rubber tube of the pneumatic tendon, m;

θ_0 − Fiber initial weaving angle, rad;

θ − Fiber instant knitting angle, rad;

ε − Contraction rate of pneumatic tendon;

D_0 − The initial diameter of the pneumatic tendon, m.

Through the pressure experiment of pneumatic tendon, the relationship between tendon contractility and tension can be determined. Further verify the correctness of the mathematical model of the pneumatic tendon. The composition of the experimental system of the pneumatic tendon is shown in Figure 3.4.

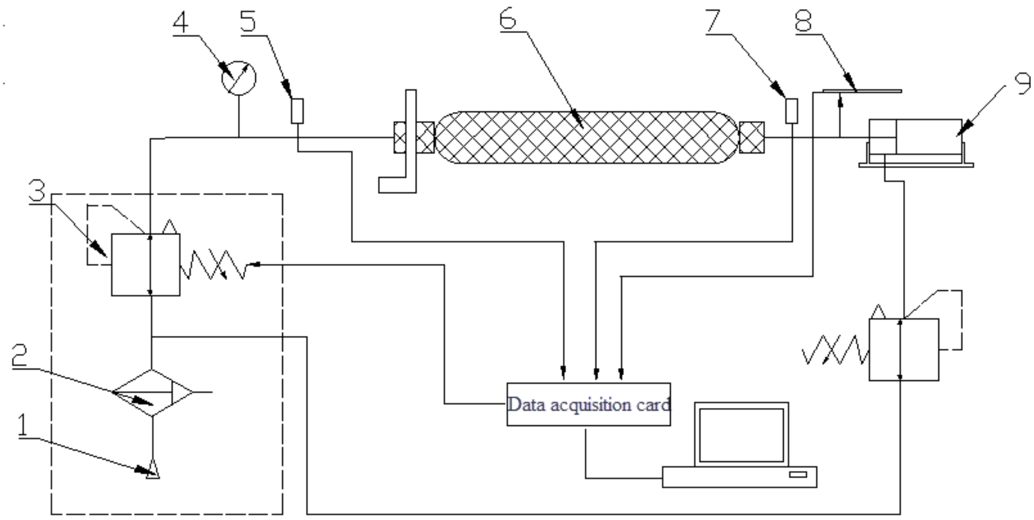

FIGURE3.4 Pneumatic Muscle Pressure Experiment Principle
1-Air Supply; 2- Filter; 3- Proportional Pressure Reducing Valve; 4-Pressure Gauge 5-Air Pressure Sensor; 6-Pneumatic Tendon; 7- Force Sensor; 8- Displacement Sensor; 9-Load Cylinder

The relationship between contractile force and systolic displacement of pneumatic tendon was obtained, as shown in figure 3.5. In order to facilitate the description of the experimental results, the vertical axis with the contraction force F said, the abscissa with the pneumatic tendon contraction rate ε to express. Under different inflation pressures, the contractile force F and the shrinkage ε of pneumatic tendon are nonlinearly quadratic. With the increase of inflation pressure, the improved model curve is getting closer to the experimental curve. It shows that the pneumatic tendon in the smaller inflation pressure is relatively strong nonlinear, with the inflatable pressure increases, the nonlinear is getting smaller and smaller. The experimental results show that the improved mathematical model of pneumatic tendon can accurately reflect the static characteristics of pneumatic tendon.

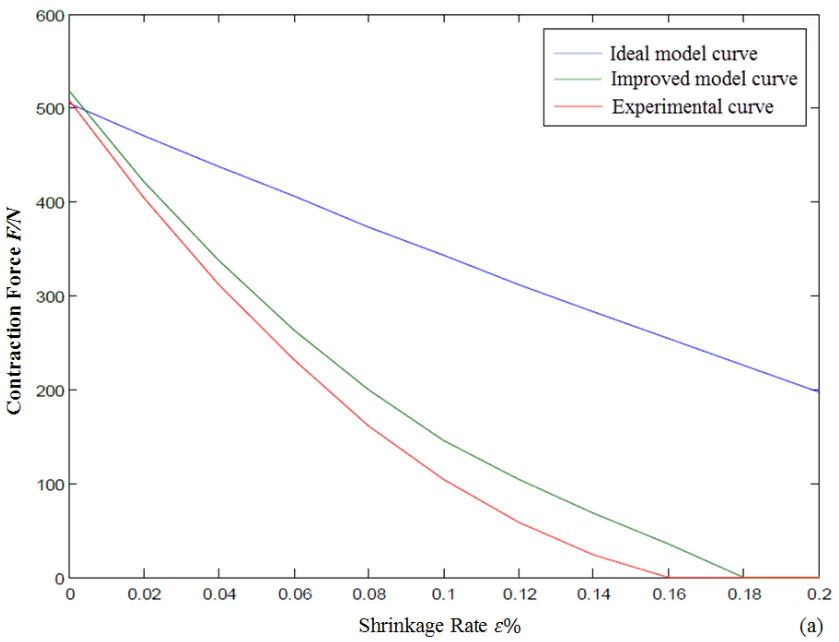

(a)

4

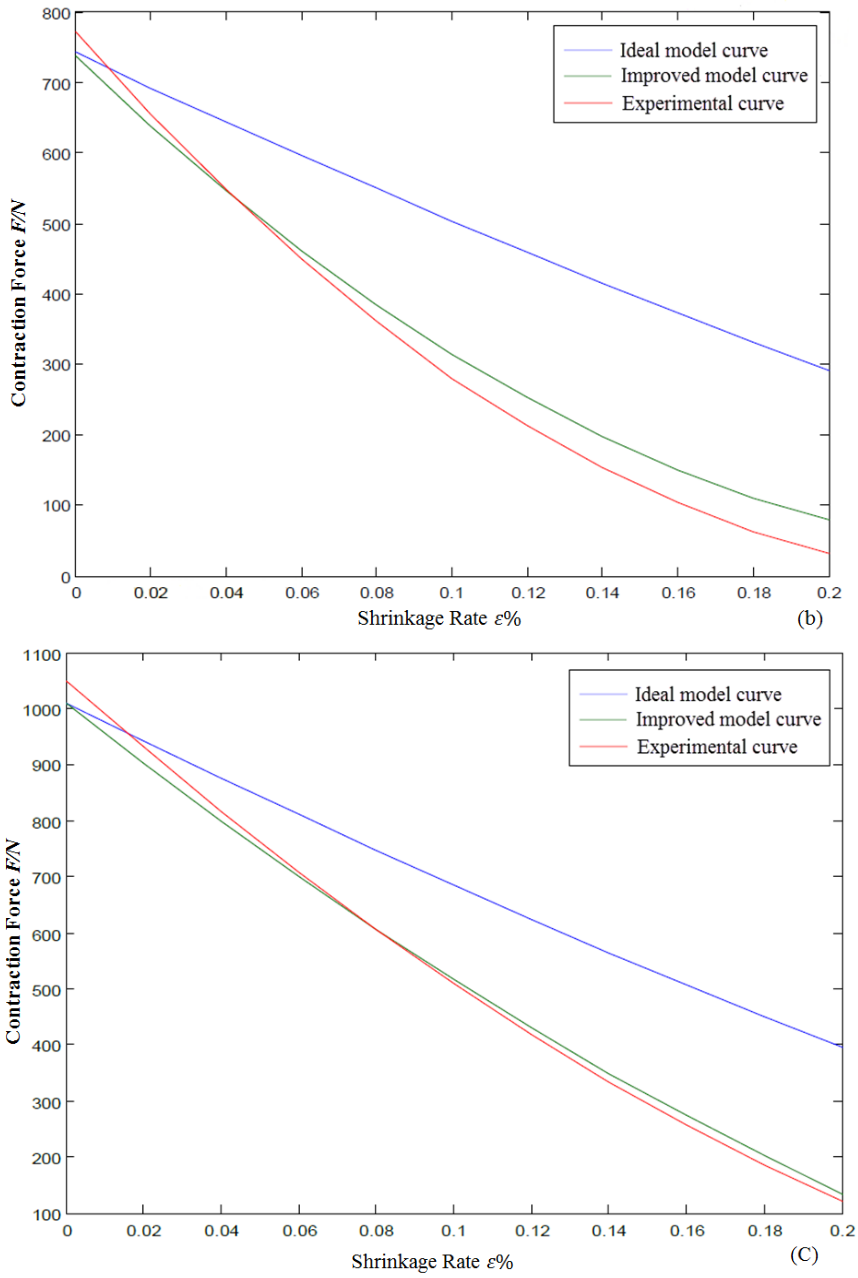

FIGURE 3.5 The Relationship between Shrinkage Rate and Contraction Force
(a) P=0.2MPa; (b) P=0.3MPa; (c) P=0.4MPa

4 DYNAMIC ANALYSIS OF INTELLIGENT PIPELINE PLUGGING DEVICE

4.1 The Mechanical Dynamics Equation of ADAMS

Mechanical dynamics is the science of studying the movement of machinery under force, or mechanically generated forces in motion. It is the theoretical basis of modern mechanical design, but also an important means to guide the mechanical design. ADAMS (Automatic Dynamics Analysis of Mechanical System) is one of the most widely used in the world of mechanical system simulation analysis software. ADAMS uses the Cartesian coordinates of the rigid body j and the Euler angles as the generalized coordinates $q_j = [x, y, z, \Psi, \theta, \varphi]_j^T$. For a system $q = [q_1^T, q_2^T, \cdots, q_n^T]^T$ with n rigid bodies, the differential equation of motion of the mechanical system is shown in Eq. (5), which is the second order algebraic differential equation [16].

$$\frac{\mathrm{d}}{\mathrm{d}t}\left(\frac{\partial T}{\partial \dot{q}}\right)^{T}-\left(\frac{\partial T}{\partial q}\right)^{T}+\alpha\varphi_{q}^{T}+\beta\theta_{q}^{T}=Q \tag{5}$$

Where T is the system kinetic energy; q is the system's generalized coordinate array; Q is the generalized force array; α is the complete constraint of the Lagrangian multiplicative array; β is the non-complete constraint of the Lagrangian multiplier array. Eq. (6) and (7) are the complete constraint equations and the no holonomic constraint equations, respectively.

$$\varphi(q,t)=0 \tag{6}$$

$$\theta(q,\dot{q},t)=0 \tag{7}$$

4.2 Model Settings

According to the model structure described in Figure 3.1, Solidworks software are used to build the assembly model, import ADAMS, and define the material properties of each component.

4.2.1 Impose constraints

After the model is imported, they need to be connected with constraint pairs to define the relative motions between objects. Common constraints are: ideal constraints, virtual constraints, high pair of constraints and motion constraints, etc. In the IPT model, the left bearing block and the push cylinder are connected by bolts, there is no relative movement between them, so add a fixed pair; the six locking sliders, which are evenly distributed in the circumferential direction, move along the dovetail groove of the cone, so they are connected by moving pairs, in which the dynamic and static friction coefficients are 0.3, 0.5, respectively; during the plugging process, the locking sliders are opened in the radial direction to form the plane pair on the surface of the cylinder. The dynamic and static friction coefficients are 0.3 and 0.5, respectively.

4.2.2 Imposed load

With the non-linear relationship between the allowable force and the contraction length ratio of the MXAM-20-AA type pneumatic tendon [17] when the air pressure of the pneumatic tendon is different, the relationship between the force and the shrinkage length ratio is different. Now, when the non-linear relationship of 0.6MPa is used as the driving force characteristic of the IPT, the fitted driving force curve is shown in Fig. 4.1 [18].

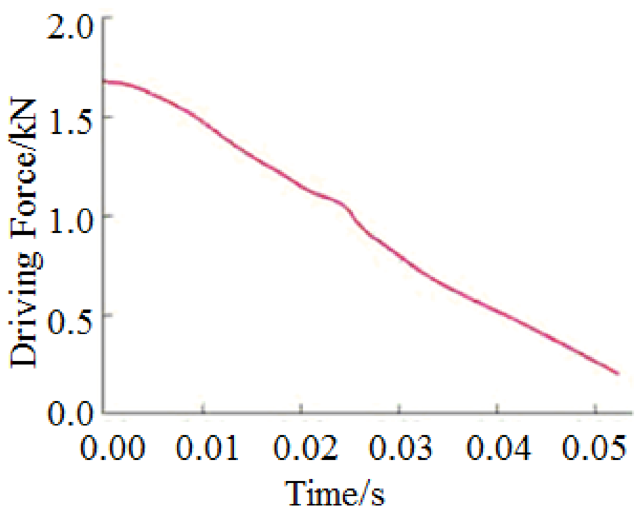

FIGURE 4.1 Driving Force Curve

4.3 Simulation Results and Analysis

Run the simulation to get the dynamic curve of the IPT. The curves of the displacement, speed and acceleration of the locking sliders in the Y and Z axes are shown in Figures 4.2 and 4.3, respectively. In the process of plugging, the speed of the locking sliders along the Y, Z axis is basically uniform changes. Due to the role of friction, acceleration at 0.013s has the jump phenomenon, which is causing speed fluctuations. The plugging operation has completed in the 0.783s, the speed quickly reduces to 0. But due to inertia, the acceleration has a greater volatility. The acceleration curve of the locking sliders is Fourier-changing, and when the frequency is 0-26Hz, the influence of the acceleration of the system is more significant, as shown in Figure 4.4.

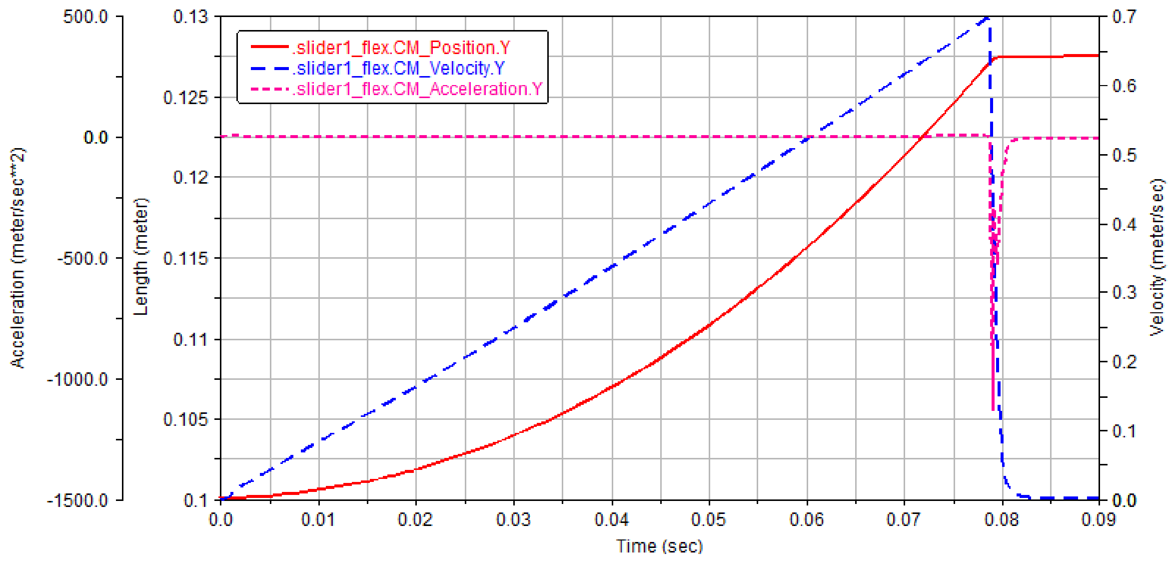

FIGURE 4.2 The Locking Sliders Displacement, Speed, Acceleration Curve along the Y Axis

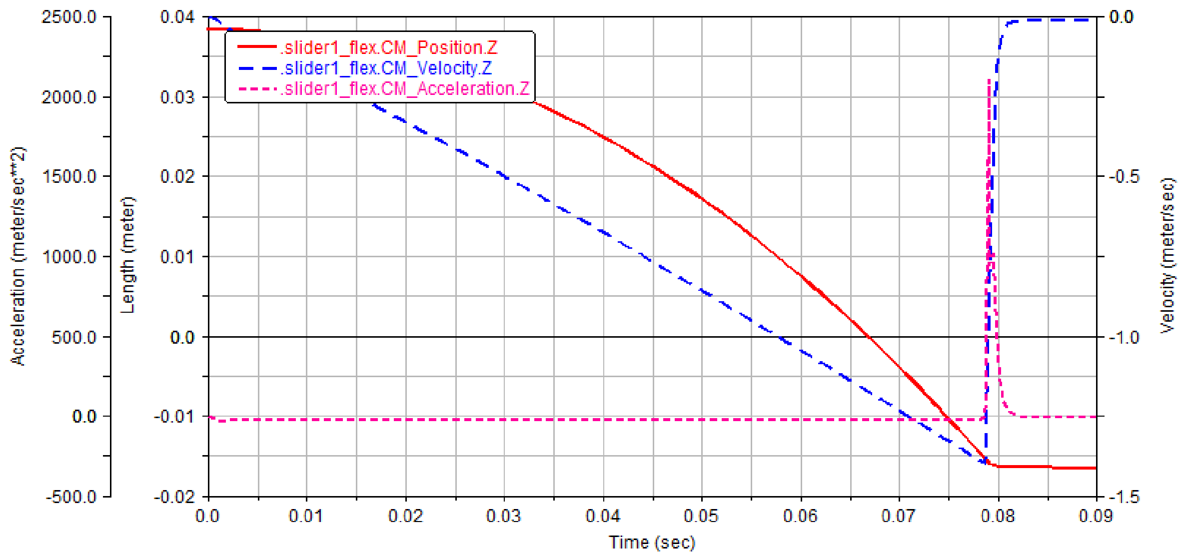

FIGURE 4.3 The Locking Sliders Displacement, Speed, Acceleration Curve along the Z Axis

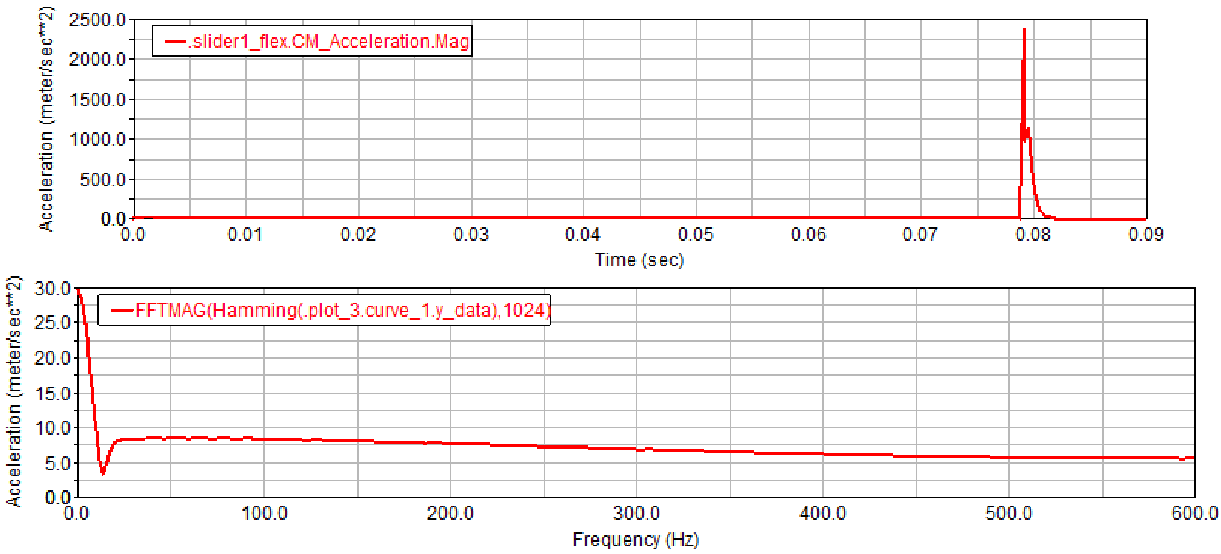

FIGURE 4.4 Fourier Changes of the Centroid Acceleration Curve of the Locking Sliders

5 DURABILITY ANALYSIS OF INTELLIGENT PIPELINE PLUGGING DEVICE

Through the durability test can be resolved the problems such as when the organization is scrapped, and when the parts is fail, which is important to understand the performance of the mechanical components.

5.1 Force Analysis of the Locking Slider

During the plugging process, the locking sliders move along the dovetail groove of the cone and come into close contact with the inner wall of pipeline, which is prone to deformation or failure, so it is subjected to durability analysis. In the process of plugging, the von mises stress; max prin. stress; max shear stress of the locking sliders at 0.0792s are as shown in 5.1(a), (b), (c), respectively. The stress values of the partial points are shown in Table 5.1. As it can be seen from the figure, the central area of the outer surface of the locking sliders are subject to greater stress and are more likely to fail.

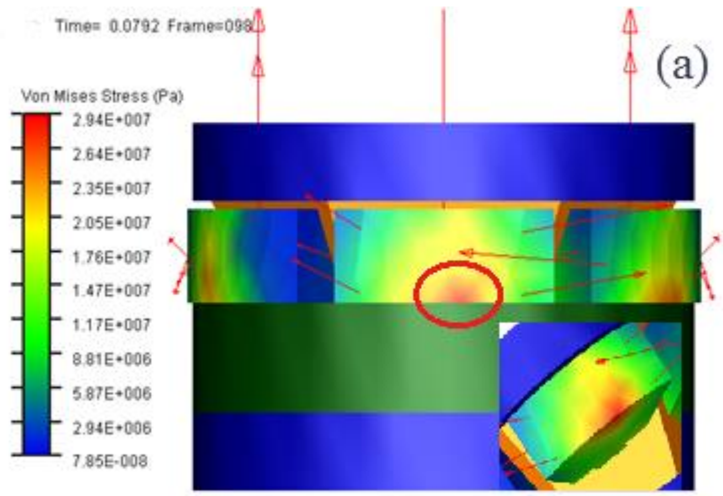

8

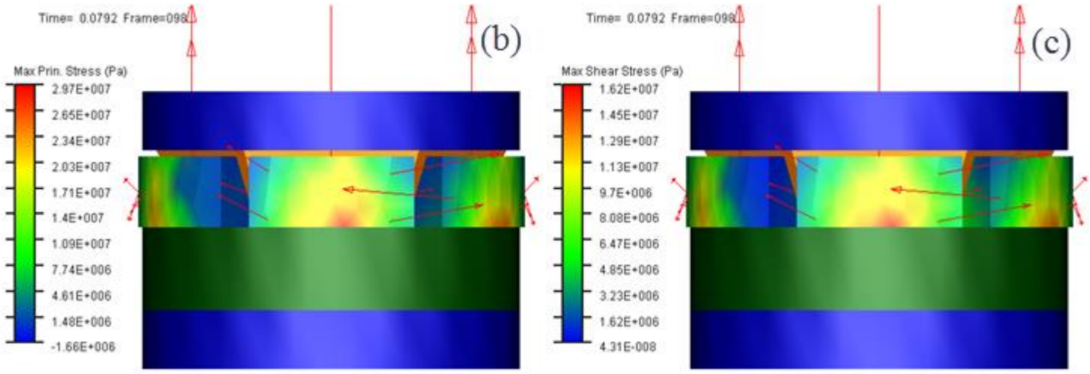

FIGURE 5.1 Force Analyses of the Locking Sliders
(a) Von Mises Stress ;(b) Max Prin. Stress ;(c) Max Shear Stress

TABLE 5.1 The Equivalent Stress Values at the Points of the Locking Sliders

Hot Spot	**Stress**	**Node**	**Time**	**Location**		
#	newton/meter^2	id	sec	X	Y	Z
1	2.94e+007	73	7.92e-002	-6.82e-003	1.29e-001	6.62e-002
2	2.53e+007	74	7.92e-002	-2.75e-003	1.29e-001	6.62e-002
3	2.50e+007	106	7.92e-002	4.58e-003	1.28 e-001	5.08 e-002
4	2.49e+007	68	7.92e-002	-7.43 e-003	1.17 e-001	6.62 e-002
5	2.29e+007	105	7.92e-002	-1.55 e-003	1.30 e-001	4.48 e-002
6	2.28e+007	101	7.92e-002	-3.61 e-003	1.29 e-001	5.02 e-002
7	2.26e+007	72	7.92e-002	1.37 e-003	1.27 e-001	6.62 e-002
8	2.04e+007	75	7.92e-002	-4.80 e-003	1.27 e-001	6.62 e-002
9	1.93e+007	108	7.92e-002	-1.56 e-003	1.30 e-001	2.30 e-002
10	1.92e+007	112	7.92e-002	-1.79 e-003	6.94e-002	3.38 e-002

5.2 Force Analysis of Inner Wall of Pipeline

With the increasing of plugging progress, the locking sliders inset the inner wall of the pipe is getting deeper and deeper and the stress on the pipe is getting bigger and bigger. The maximum stress of the pipe appears at the pipe where the locking sliders are embedded, extending from the inner wall of the pipe to the outer wall of the pipe. Figure 5.2 shows the change in the maximum stress of the pipe wall during the blockage process.

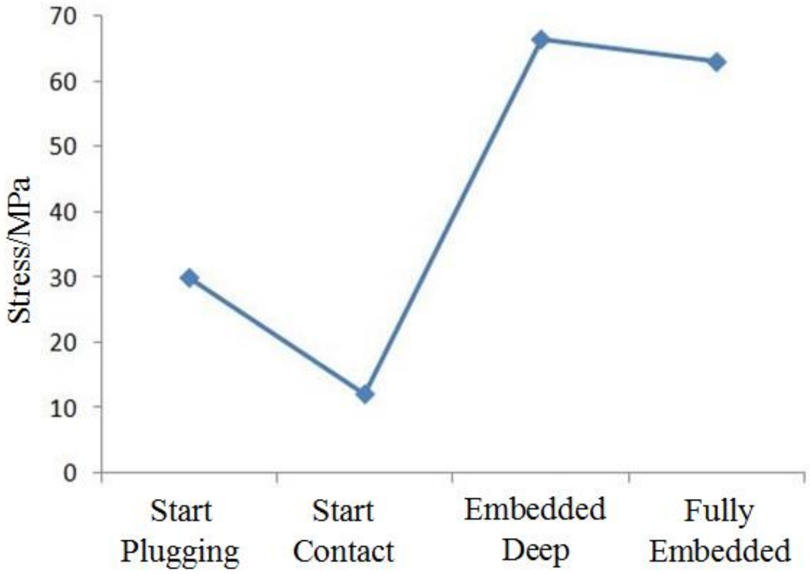

FIGURE 5.2 The Maximum Stress Change Curve

As shown in the figure 5.2, the maximum stress applied by the pipe at the beginning of the plug is about 30 MPa, the maximum stress at the beginning of the locking sliders inset the inner wall of pipeline is 12.22 MPa, the maximum stress when the locking sliders into the inner wall of the pipe deep is 66.45MPa, the maximum stress when the locking sliders are fully embedded in the inner wall of the pipe is 63 MPa. From the beginning of the plug to the locking sliders contact with the inner wall of the pipe, the stress has decreased, when embedded deep, the stress value to the maximum. The stress after plugging is 63MPa, the limit of the pipe yields 200Pa, so the stress of the pipe wall is within the safe range.

6 CONCLUSION

With the development of petrochemical industry, the safety and environmental protection required by the pipeline maintenance, repair, renovation and other projects are becoming much stricter. Therefore, the further development of the intelligent plugging process and key equipment will be the key to whether the technology can be extended to a wider range of applications.

Based on the analysis of the mechanical structure of the existing intelligent plugging device, this paper proposes to use the pneumatic tendon instead of the hydraulic cylinder to provide the plugging power, and design a kind of intelligent plugging device suitable for high pressure and small aperture oil and gas pipeline. The dynamic simulation and durability analysis are carried out, and it is concluded that in the process of plugging, the locking sliders are subjected to defects such as large impact, instability and stress concentration, etc. To solve these problems, make the sealing ring on the outer surface of the locking slider; drill the dovetail groove on the top surface of the push cylinder to reduce the lateral movement between the locking slider and the push cylinder to make the plugging process more stable. Which can provide reference for the design and optimization of IPT.

ACKNOWLEDGMENTS

This work was financially supported by the National Natural Science Foundation of China (Grant No. 51575528), the Scientific Research Foundation of the Education Ministry for Returned Chinese Scholars (China), the State Key Laboratory for Coal Resources and Safe Mining, China University of Mining and Technology (No. SKLCRSM10KFB04), and the Science Foundation of China University of Petroleum, Beijing (No. YXQN-2014-02).

REFERENCES

1. Liu Chenhou, Pan Dongnin, Wu Yishan. Review of Submarine Pipeline Maintenance. China Offshore Oil and Gas (in Chinese), 2004, 16-1, pp. 59-62.
2. Ma Ning, Zhang Juan. Pipeline dimensional repair technology of China National Petroleum. Chemical Management (in Chinese), 2013, 4, pp. 21-23.
3. Jiang Longqiang. Present Situation and Development of Pipeline Sealing Repair Technology. Inner Mongolia Petrochemical Industry (in Chinese), 2011, 2, pp. 100-103.
4. Zhang Shimin, Min Xutao, Wang Guochao, et al. Method and Technology Progress of Oil Pipeline Maintenance. Oil and Gas Storage and Transportation (in Chinese), 2014, 33-11, pp. 1180-1185.
5. Zhang Shimin, Tan Guibin, Zhu Xiaoxiao, et al. Technical Progress of Maintenance Repair of Oil and Gas Pipeline. Petroleum Machinery (in Chinese). 2011, 39-10, pp. 174-178.
6. Zhang Shimin, LI Yanmin, Ma Yongming, et al. High Pressure Intelligent Plugging Technology in Tube. Oil & Gas Storage and Transportation (in Chinese). 2009, 28-6, pp.59-61.
7. Ma Ming, Zhao Hong, He Teng. ADAMS-based Kinetic Research on the Locking Mechanism of Pipeline Plugging Device. China Petroleum Machinery (in Chinese), 2014, 42-4, pp. 101-105.
8. Nieckele AO, Braga AMB, Azevedo LFA. Transient pig motion trough gas and liquid pipelines. ASME J Energy Resour. 2001; 12(3):260–9. doi:10.1115/1.1413466.
9. Yeung HC, Lima PCR. Modeling of pig assisted production methods. J Energy Resour Technol Trans ASME. 2002; 124(3):8–13. doi:10.1115/1.1446474.
10. Xu XX, Gong J. Pigging simulation for horizontal gas-condensate pipelines with low-liquid loading. J Pet Sci Eng. 2005; 48:272–80. Doi: 10.1016/j. petrol.2005.06.005.
11. Saeidbakhsh M, Rafeeyan M, Ziaei-rad S. Dynamic analysis of small pigs in space pipelines. Oil Gas Sci Technol. 2009; 64(2):155–64. Doi: 10.2516/ogst: 2008046.
12. Lesani M, Rafeeyan M, Sohankar A. Dynamic analysis of small pig through two and three dimensional liquid pipeline. J Appl Fluid Mech. 2012; 5-2, pp.75–83.
13. Zeng D, Deng K, Lin Y. Theoretical and experimental study of the thermal strength of anticorrosive lined steel pipes. Pet Sci. 2014; 11(3):417–23. Doi: 10.1007/s12182-014-0356-z.
14. Minami K, Shoham O. Pigging dynamics in two-phase flow pipelines: experiment and modeling. SPE Prod Facil. 1995; 10(4):225–32. Doi: 10.2118/26568-PA.

15. Hong Zhao, Yi-Xin Zhao, Zhi-Hui Ye. Interactions between the fluid and an isolation tool in a pipe: laboratory experiments and numerical simulation. Petroleum Science. 2016, 13, pp.746–759.
16. He Xiong. Analysis of ADAMS Dynamic Simulation Algorithm and Parameter Setting. Drive System Technique (in Chinese), 2005, 3, pp. 27-30.
17. FESTO. Fluidic Muscle [EB/OL]. http://wenku.baidu.Com/view/ 911cfd2b3169a 4517723a341. Html.
18. Guo Weidong. Virtual Prototyping Technology and ADAMS Application Examples Tutorial. Beijing: Beijing University Press (in Chinese), 2008.

